MOLECULAR AND CELLULAR BIOLOGY, Dec. 2006, p. 9045–9059 Vol. 26, No. 23
0270-7306/06/$08.00+0 doi:10.1128/MCB.00248-06

The LRS and SIN Domains: Two Structurally Equivalent but Functionally Distinct Nucleosomal Surfaces Required for Transcriptional Silencing▽

Christopher J. Fry,[1]† Anne Norris,[2]† Michael Cosgrove,[3] Jef D. Boeke,[2] and Craig L. Peterson[1]*

Program in Molecular Medicine, University of Massachusetts Medical School, Worcester, Massachusetts 01605[1]; Department of Molecular Biology and Genetics and High Throughput Biology Center, The Johns Hopkins University, Baltimore, Maryland 21205[2]; and Department of Biology, Syracuse University, 406D Lyman Hall, 108 College Place, Syracuse, New York 13244[3]

Received 9 February 2006/Returned for modification 3 March 2006/Accepted 14 September 2006

Genetic experiments have identified two structurally similar nucleosomal domains, SIN and LRS, required for transcriptional repression at genes regulated by the SWI/SNF chromatin remodeling complex or for heterochromatic gene silencing, respectively. Each of these domains consists of histone H3 and H4 L1 and L2 loops that form a DNA-binding surface at either superhelical location (SHL) ±2.5 (LRS) or SHL ±0.5 (SIN). Here we show that alterations in the LRS domain do not result in Sin⁻ phenotypes, nor does disruption of the SIN domain lead to loss of ribosomal DNA heterochromatic gene silencing (Lrs⁻ phenotype). Furthermore, whereas disruption of the SIN domain eliminates intramolecular folding of nucleosomal arrays in vitro, alterations in the LRS domain have no effect on chromatin folding in vitro. In contrast to these dissimilarities, we find that the SIN and LRS domains are both required for recruitment of Sir2p and Sir4p to telomeric and silent mating type loci, suggesting that both surfaces can contribute to heterochromatin formation. Our study shows that structurally similar nucleosomal surfaces provide distinct functionalities in vivo and in vitro.

The nucleosome constitutes the central structure of chromatin and comprises two chains each of histones H2A, H2B, H3, and H4, which are assembled into a histone octamer and around which 147 bp of DNA is wrapped ~1.7 times (18). Previous studies identified two nucleosomal surfaces, SIN (switch independent) and LRS, which are important for transcriptional repression in *Saccharomyces cerevisiae* (13, 24, 33). These domains lie at opposite ends of the crescent-shaped, quasisymmetric H3-H4 heterodimer. Histone residues altered in *sin* mutants or in five of the *lrs* mutant alleles can be structurally superimposed by a rotation of 180° around a symmetry axis at superhelical location (SHL) ±1.5. Thus, the two "ends" of each (H3-H4) "crescent" are structurally equivalent yet organize different regions of the DNA (Fig. 1). Alterations within these two clusters relieve distinct forms of transcriptional repression: the *sin* mutant alleles partially bypass the need for the SWI/SNF chromatin remodeling complex (13, 24, 33), and *lrs* mutant alleles lead to a loss of repression of genes placed in transcriptionally silent regions of the genome (e.g., the ribosomal DNA locus or telomeres) (24, 33).

Sin⁻ alterations in histones H3 and H4 were identified in yeast genetic screens for mutations that alleviated the transcriptional defects associated with inactivation of the SWI/SNF chromatin remodeling complex (13, 24, 33). In addition, the expression of Sin⁻ histones leads to derepression of the *PHO5* gene in high-phosphate conditions even in wild-type yeast, suggesting that Sin⁻ histones also weaken more general, nucleosome-mediated repression of basal transcription (38). *sin* mutations within genes encoding histones H3 or H4 lead to single-amino-acid changes that cluster around the nucleosomal dyad axis (SHL ±0.5) (13, 18). Because interactions between DNA and the histone octamer are strongest at the dyad region of the nucleosome, disruption of histone-DNA contacts in this region may be the rate-limiting step in nucleosomal dissociation and sliding (20). X-ray structures of Sin⁻ mononucleosomes have demonstrated that Sin⁻ versions of histone H4 or H3 do not affect the overall structure of the nucleosome but rather disrupt only a small percentage of histone-DNA contacts (22). These subtle changes in histone-DNA interactions provide a likely explanation for why Sin⁻ mononucleosomes dissociate at significantly lower ionic strength and why they have a lower energy barrier towards temperature-induced nucleosome repositioning ("sliding") (7, 15, 22). In contrast, nucleosomal arrays reconstituted with Sin⁻ versions of histone H4 do not exhibit altered positioning of nucleosomes, nor do Sin⁻ nucleosomes within these arrays show altered accessibility to restriction enzymes (12). Interestingly, these Sin⁻ nucleosomal arrays show defects in formation of condensed, 30-nm-like fibers. This folding defect mimics the loss of condensation due to removal of the histone N-terminal domains (8, 12). These results have led to two models for how Sin⁻ histones might compensate for inactivation of SWI/SNF in vivo: (i) the enhanced thermal mobility of Sin⁻ mononucleosomes makes chromatin remodeling unnecessary, and (ii) the unfolded state of Sin⁻ nucleosomal arrays may mimic the "remodeled state" of chromatin acted on by SWI/SNF. These models may not be mutually exclusive, as the enhanced mobility of Sin⁻ nucleosomes may inhibit chromatin condensation.

In contrast to the Sin⁻ alterations, little is known about the

* Corresponding author. Mailing address: Program in Molecular Medicine, University of Massachusetts Medical School, Biotech 2, Suite 210, Worcester, MA 01605. Phone: (508) 856-5858. Fax: (508) 856-5011. E-mail: Craig.Peterson@umassmed.edu.
† These authors contributed equally to this work.
▽ Published ahead of print on 2 October 2006.

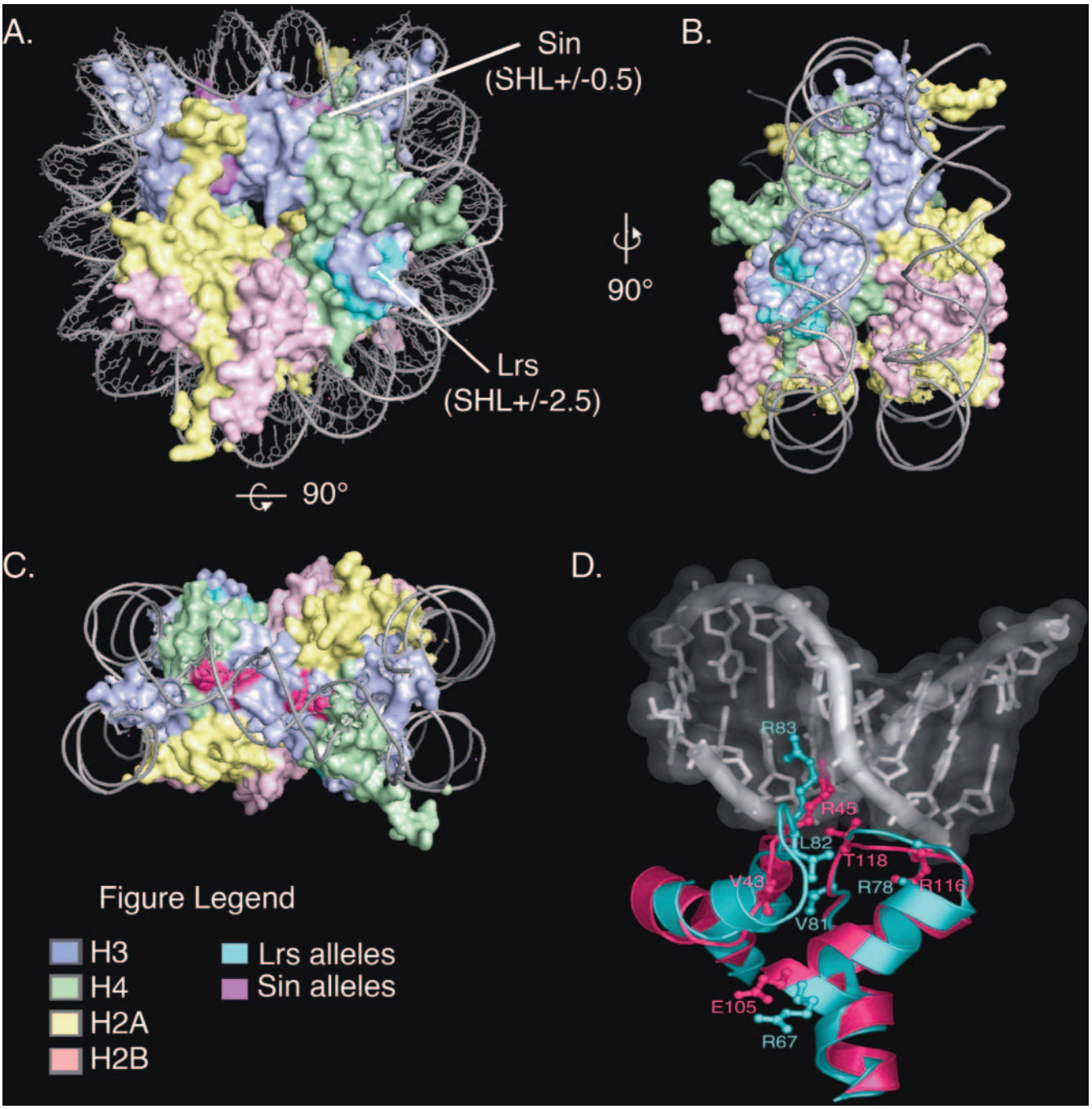

FIG. 1. Mapping of Sin and Lrs alterations onto the surface of the yeast nucleosome core particle. (A) Surface representation of the yeast nucleosome core particle (Brookhaven PDB 1ID3) viewed down the DNA superhelix axis (disk surface). Sin alleles map to SHL ±0.5, and the LRS alleles map to SHL ±2.5. (B) A 90° rotation about the *x* axis of the image shown in panel A shows the relationship of LRS alleles to the DNA. (C) A 90° rotation about the *y* axis of the image shown in panel A shows the relationship of the Sin alleles to the DNA. (D) An overlay of the Sin and Lrs histone fold domains demonstrates their structural similarities.

biochemistry of Lrs$^-$ histones. The *lrs* mutants were identified in an unbiased yeast genetic screen for mutations that alleviate silencing of an RNA polymerase II (Pol II) reporter gene that had been inserted into the ribosomal DNA locus (24). Additionally, the *lrs* mutant alleles were found to alleviate transcriptional silencing at telomeres and, to a lesser extent, the silent mating type loci (*HM* loci). Given the striking structural similarity of the LRS and SIN domains, it is attractive to hypothesize that these two surfaces fulfill similar functions. Here we have compared the in vivo and in vitro phenotypes of Lrs$^-$ and Sin$^-$ histone alterations. We find that *lrs* mutants do not exhibit Sin$^-$ phenotypes, nor do *sin* mutants exhibit defects in ribosomal DNA silencing. In contrast to Sin$^-$ versions of H4, we find that an Lrs$^-$ version of histone H3 does not disrupt

TABLE 1. Yeast strains

Strain or plasmid	Genotype and characteristics	Reference or source
Strain		
JPY12	*MAT***a** *his3Δ200 leu2Δ1 lys2Δ0 trp1Δ63 ura3-167 met15Δ0 ade2*::*his RDN1*::*mURA3*/*HIS3 RDN1*::*Ty1-MET15 TELV*::*ADE2 hht2-hhf2*::*hygMX hht1-hhf1*::*natMX* pJP11 (*LYS2 CEN HHT1-HHF1*)	24
EMHY 234	*MAT***a** *dot1*Δ::Kan^r, isogenic to JPY12	E. M. Hyland and J. D. Boeke, unpublished
UCC3505	*MAT***a** *ura3-52 lys2-801 ade2-101 trp1Δ63 his3Δ200 leu2Δ1 ppr1*::*HIS3 adh4*::*URA3-TEL-V11L VR-ADE-TEL*	30
ANY34	UCC3505 *hht2-hhf2*::*hygMX hht1-hhf1*::*natMX* pJP11 (*LYS2 CEN HHT1-HHF1*)	A. Norris and J. D. Boeke, unpublished
CY232	*MATα HO-lacZ trp1 ura3 leu2 met*$^-$ *his*$^-$	I. Herskowitz
CY240	*MAT***a** *HO-lacZ swi1*Δ::*LEU2*, congenic to CY232	I. Herskowitz
CY1109	*MAT***a** *sir1*Δ::Kan^r, isogenic to JPY12	
CY1113	*MAT***a** *sir4*Δ::Kan^r, isogenic to JPY12	
CY1045	JPY12 with pDM18 (*TRP1-CEN-hht2* [*K79E*]-*HHF2*)	
CY1110	*MATt***a** *sir1*Δ::Kan^r, isogenic to CY1045	
CY1044	JPY12 with pDM18 (*TRP1-CEN-hht2* [*K79R*]-*HHF2*)	
CY1111	*MAT***a** *sir1*Δ::*Kan*^{r}, isogenic to CY1044	
CY1047	JPY12 with pDM18 (*TRP1-CEN-hht2* [*R83A*]-*HHF2*)	
CY1112	*MAT***a** *sir1*Δ::Kan^r, isogenic to CY1047	
CY1169	JPY12 with pDM18 (*TRP1-CEN-HHT2-hhf2* [*R45H*])	
CY1278	*MAT***a** *sir1*Δ::Kan^r, isogenic to CY1169	
CY1171	JPY12 with pDM18 (*TRP1-CEN-HHT2-hhf2* [*V43I*])	
CY1279	*MAT***a** *sir1*Δ::Kan^r, isogenic to CY1171	
Plasmid		
pDM18	*TRP1 CEN HHT2-HHF2*	6
pJP11	*LYS2 CEN HHF1-HHT1*	24

formation of condensed, 30-nm-like fibers in vitro. Our genetic and biochemical studies indicate that these two nucleosomal surfaces have distinct functionalities in vitro and in vivo.

MATERIALS AND METHODS

Strains, media, and plasmids. All yeast strains are described in Table 1. Yeast media were exactly as described previously (31), except that 0.8 mM adenine was added to Pb^{2+}-containing medium. The drugs clonNAT and hygromycin were used as described previously (9).

The strain ANY34, in which all four histone H3 and H4 genes were disrupted, was constructed, and all other strains are summarized in Table 1. The reporter strain for telomeric silencing, ANY34, was generated from strain UCC3505 containing the telomeric *URA3*- and *ADE2*-silencing reporters. The drug marker *NATMX4* was amplified from the plasmid pAG25 (9) using *HHT1-HHF1*-flanking sequence primers JB2775 and JB2776 (primer sequences are available upon request). *HPHMX4* was amplified from pAG32 (9) using *HHT2-HHF3*-flanking sequence primers JB2777 and JB2778. Using these PCR products, we replaced *HHT1-HHF1* with *NATMX4*, transformed it with plasmid pJP11, and then replaced *HHT2-HHF2* with *HPHMX4*.

Plasmids pJP11 and pDM18 contain wild-type *HHT1-HHF1* and *HHT2-HHF2* regions, respectively, and were described previously (24). pRS416 derivatives of wild-type and mutant *HHT2* alleles were constructed by PCR amplification of wild-type and mutant *HHT2* alleles in pDM18 (24) using the following primers: upstream (5′-CTC ACT AAA GGG AAC AAA AG-3′) and downstream (5′-CTT GTA CTT AGA ATT CCT ACA TAC GCA CAA ACA CG-3′). PCR fragments were then cloned into the XmaI and EcoRI sites of pRS416 (Stratagene). The pRS416 derivative of *hhf2* R45C was cloned by Quikchange XL site-directed mutagenesis (Stratagene) using pRS416-*HHF2* plasmid (CP530). pDM18 derivatives of the *sin* mutant alleles were cloned by Quikchange XL site-directed mutagenesis (Stratagene) using pDM18 containing wild-type *HHT2-HHF2* alleles (24). pDM18 derivatives of all other wild-type and mutant *HHT2* and *HHF2* alleles have been described previously (24).

β-Galactosidase filter assay. Suppression of *swi*/*snf* defects in *HO-lacZ* transcription was assayed by transforming histone H3 and H4 alleles (pRS416 derivatives) into strains CY232 (*SWI*$^+$) and CY240 (*swi1*Δ) that contain an *HO-lacZ* reporter gene. Four clones for each mutant yeast strain were patched onto synthetic complete (SC) plates lacking uracil (SC-Ura) and incubated overnight at 37°C. Yeast patches were then replica plated onto a Whatman 50 filter placed on a second SC-Ura plate and incubated overnight at 37°C. Relative expression levels of the *HO-lacZ* reporter gene in each strain were demonstrated using a β-galactosidase filter assay, as described previously (13).

Reverse transcription-PCR (RT-PCR) analysis of *HO-lacZ* and *PHO5* expression levels. *PHO5* transcriptional repression under high-phosphate conditions and *HO-lacZ* expression were assayed in JPY12 transformed with pDM18 derivatives of histones H3 and H4. Cells were grown to mid-log phase in yeast extract-peptone-dextrose (YEPD) medium at 30°C, and 10 ml of cell culture was harvested for RNA by extraction with hot acidic phenol. First-strand cDNA synthesis was performed using 2.5 μg total RNA, SuperScript II RNase H$^-$ reverse transcriptase (Invitrogen), and 2 pmol each of *PHO5*, *HO-lacZ*, or *ACT1* downstream primers, following the manufacturer's instructions. Subsequently, semiquantitative, ^{32}P-labeled PCR was performed using 2 μl of the first-strand cDNA reaction, *Taq* Polymerase (Promega), and gene-specific primer sets to determine the relative levels of *PHO5*, *HO-lacZ*, and *ACT1* mRNA for each mutant strain. After 14 cycles (for *ACT1*) or 22 cycles (for *PHO5* and *HO-lacZ*) of amplification, PCR products were electrophoresed on 10% acrylamide. Signals were quantified using a PhosphorImager and ImageQuant v4.2 (Molecular Dynamics). For quantification, *PHO5* expression levels were normalized to *ACT1* expression, and *PHO5* expression in the wild-type strain was set to 1.0. Data shown in Fig. 2B are the average of four independent experiments with standard deviations. Primer sequences are available upon request.

Recombinant histone and histone octamer preparation. *Xenopus laevis* histone H3 R83A was cloned from pET3D1-Histone H3 C28S (CP1035) after Quikchange XL site-directed mutagenesis (Stratagene). Clones were confirmed by sequence analysis using the Prism Ready Reaction DyeDeoxy Terminator Cycle Sequencing kit v3.0 (Perkin Elmer) and transformed into BL21(DE3) cells (Invitrogen).

Recombinant *X. laevis* histones were purified from inclusion bodies of BL21 cells (19). Proteins were >99% pure after two steps of chromatography. Following chromatography, histones were dialyzed against water to remove urea and lyophilized. Wild-type and mutant histone octamers were reconstituted and purified as described previously (12). Histone octamers were deposited onto the 208-11 DNA template by salt dialysis (11), and deposition was confirmed by EcoRI cleavage of nucleosomal arrays (Fig. 3A) (12).

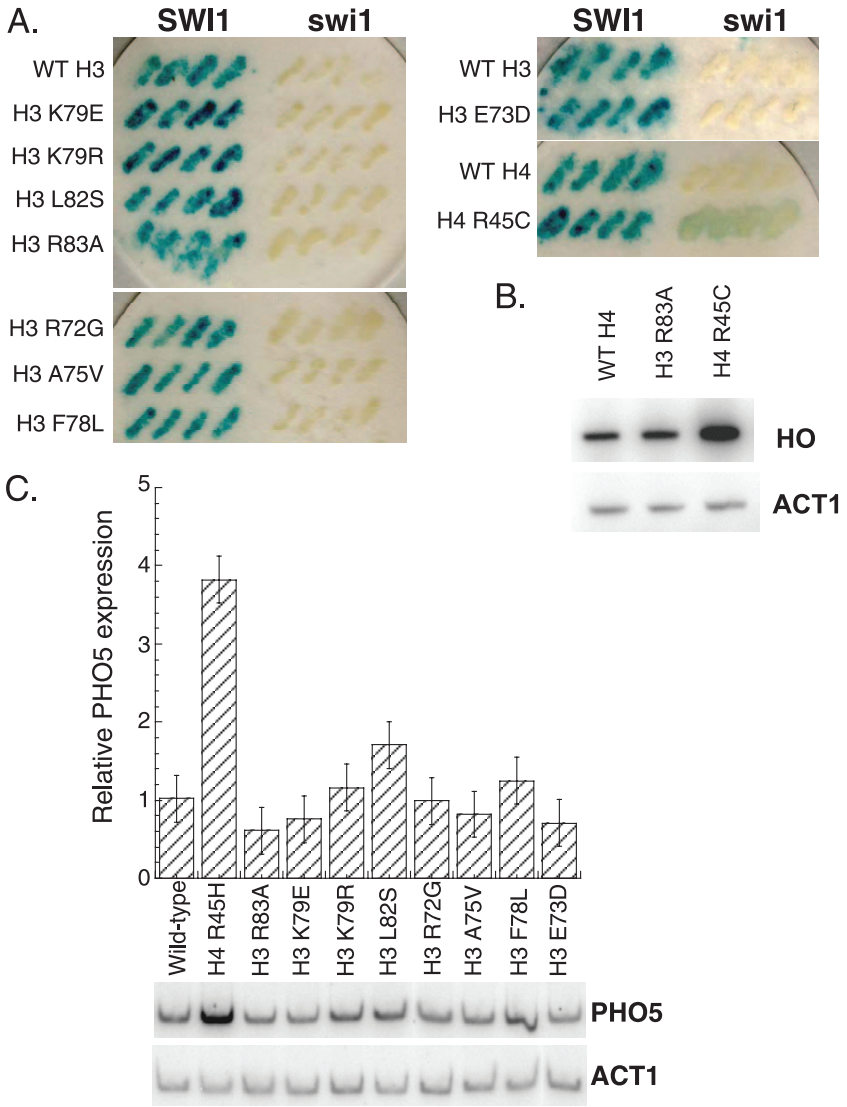

FIG. 2. Lrs$^-$ alterations do not show a Sin$^-$ phenotype in vivo. (A) Lrs$^-$ alterations do not suppress *swi/snf* defects in *HO-lacZ* transcription. Strains CY232 (*SWI*) and CY240 (*swi1*), both containing an *HO-lacZ* reporter gene, were transformed with plasmids expressing either wild-type or Lrs$^-$ histone H3 or the Sin$^-$ histone H4-R45C. Four clones of each were grown on SC-Trp plates, and *HO-lacZ* reporter gene expression was analyzed using a β-galactosidase filter assay. (B) Relative levels of *HO-lacZ* and *ACT1* gene expression in panel A were determined by RT-PCR for an *swi1*Δ strain (CY240) transformed with plasmids expressing either wild-type histone H4, histone H3-R83A, or histone H4-R45C. Similar results were observed for strains expressing other Lrs$^-$ histones. (C) Lrs$^-$ alterations do not lead to derepression of *PHO5* gene expression in high-phosphate media. JPY12 cells expressing either wild-type, Lrs$^-$, or Sin$^-$ histones as the sole source of histone H3 or H4 were grown to mid-log phase in YEPD medium and harvested for RNA. The level of *PHO5* and *ACT1* gene expression was analyzed by RT-PCR. *PHO5* expression was normalized to *ACT1* expression in each strain, with expression levels in the wild-type strain set to 1.0. The bottom panels show raw data from a representative experiment. Quantified data are graphed above and reflect the average of four independent experiments with standard deviations. WT, wild type.

Sedimentation velocity analysis. Sedimentation velocity experiments were performed in a Beckman Optima XL-I analytical ultracentrifuge using scanner optics at 260 nm. Samples were equilibrated at 20°C under vacuum for at least 1 h prior to sedimentation at 25,000 × *g* in a 60 Ti rotor. Boundaries were analyzed by the method of van Holde and Weischet (36) using UltraScan version 4.0 for Unix. Data were plotted as boundary fraction (*y* axis) versus $S_{20,w}$ (sedimentation corrected to water at 20°C) to yield the G(s) distributions (Fig. 3B). Analyses were performed three times, and data are representative of a single experiment.

Silencing assays. Silencing strength in the ribosomal DNA (rDNA) was assessed with the *mURA3/HIS3* reporter by serial dilution on SC-His medium to prevent elimination of the rDNA reporter containing 0.1% 5-fluoroorotic acid (5-FOA) to assay down-regulation of rDNA::*mURA3*. Silencing strength of the telomeric DNA was assayed by serial dilution on SC-Ura. Serial dilutions were performed as follows. Cells were scraped from the plates and resuspended in 100 μl of sterile water. The cell suspension was normalized to an A_{600} reading of 0.5 and then serially diluted in 5-fold or 10-fold increments; 5 μl of each dilution was spotted onto either nonselective or selective agar plates using a 12-channel pipette. Plates were incubated for 2 to 5 days.

Colony color silencing assays. rDNA silencing was also assayed using the *MET15* color assay. Strains to be tested were plated onto lead (MLA) plates to give approximately 100 to 200 colonies per plate. The plates were incubated at 30°C for 8 days and then photographed. Telomeric silencing was also assayed using the *ADE2* color assay. Strains to be tested were plated onto SC-Trp plates to give approximately 100 to 200 colonies per plate. The plates were incubated at 30°C for 3 days and then were incubated at 4°C for 3 days and photographed.

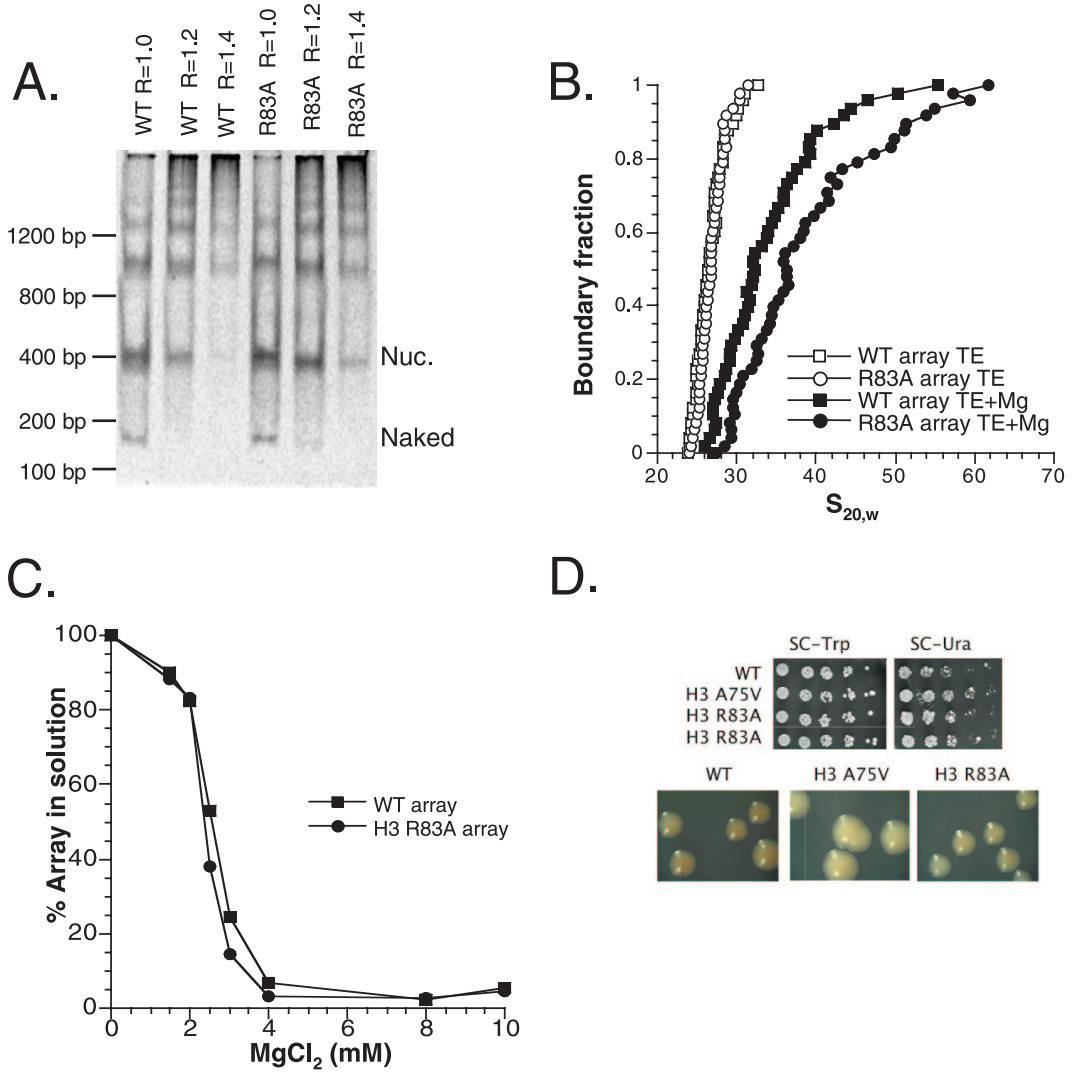

FIG. 3. Lrs$^-$ alterations do not disrupt nucleosomal array folding in vitro. Histone octamers reconstituted from recombinant histones H2A, H2B, H4, and either wild-type H3 or H3-R83A were deposited onto 208-11 DNA templates by salt dialysis. (A) R83A Lrs$^-$ nucleosomes are indistinguishable by native PAGE. Arrays harboring either the wild type or the Lrs$^-$ R83A version of histone H3 were cleaved with EcoRI, electrophoretically separated on a native 4% PAGE, and stained with ethidium bromide. The mononucleosome (Nuc) and naked DNA (Naked) bands are indicated. (B) R83A Lrs$^-$ nucleosomal arrays show normal intramolecular, salt-dependent folding as shown by sedimentation velocity analysis of 208-11 arrays in the presence or absence of Mg^{2+}. The G(s) distributions are depicted for the indicated arrays sedimented in either TE (10 mM Tris [pH 8.0], 0.25 mM EDTA) or TE with 1.75 mM $MgCl_2$. $S_{20,w}$ is the sedimentation coefficient corrected to water at 20°C. (C) Intermolecular oligomerization is not altered by the histone H3-R83A mutation. Nucleosomal arrays were incubated in TE with varying concentrations of $MgCl_2$ at room temperature for 15 min, followed by centrifugation in a microcentrifuge at 14,000 × *g* for 10 min. The percentage of array remaining in the supernatant is plotted as a function of $MgCl_2$ concentration. (D) rDNA silencing of the *lrs* mutant allele H3-R83A was determined by assaying for growth on SC-Ura to measure expression of the *mURA*/*His* reporter and plating on Pb^{2+}-containing media to assay expression of *MET15* reporter, both integrated into the rDNA locus. WT, wild type. R, ratio.

Western blot analysis. Histone H3 K79 dimethylation, H3 K79 trimethylation, total histone H3, Sir2p, and Sir4p levels were analyzed in JPY12 transformed with pDM18 derivatives of histone H3 and H4. Cells were grown to mid-log phase in YEPD medium at 30°C, and 10 ml of cell culture was pelleted, rinsed with TBS (20 mM Tris [pH 7.4], 150 mM NaCl), and resuspended in 150 μl of 3× Laemmli buffer. Each cell lysate was combined with 300 μl glass beads in a 1.5-ml Eppendorf tube and vortexed at maximal speed for 10 min at 4°C. The cell lysates were then heated for 2 min at 95°C and clarified by centrifugation, and 7 μl of cell lysate was used for sodium dodecyl sulfate-polyacrylamide gel electrophoresis (SDS-PAGE), followed by Western blot analysis with anti-histone H3 dimethyl K79 (Upstate 07-366), anti-histone H3 trimethyl K79 (Abcam 2621), anti-histone H3 (Cell Signal Technology 9715), anti-Sir2p (sc-6666), anti-Sir4p (sc-6671), and anti-TBP (M. Green, University of Massachusetts Medical School) antibodies. Experiments were performed at least twice, and data are representative of a single experiment.

In vitro Dot1 methylation assay. Recombinant Dot1 and yeast nuclear extracts were purified as previously described (37), except that the extracts were made from a *dot1*Δ derivative of JPY12. Nuclear extract concentrations were determined by measuring the spectrophotometric absorbance at 260 and 280 nm, and concentrations were normalized by dilution in a buffer containing 20 mM HEPES (pH 7.9), 400 mM NaCl, 2 mM $MgCl_2$, 0.1% NP-40, 2.5 mM 2-mercaptoethanol, and 10% glycerol. Assays were carried out by adding 1 μl of the normalized nuclear extract to a reaction containing 1 μg of purified recombinant Dot1p, 2 μCi of *S*-adenosyl-L-[*methyl*-^{3}H]methionine, 50 mM Tris-Cl (pH 7.9), 1 mM EDTA, 0.5 mM EGTA for a total volume of 15 μl. Reactions were incubated at 30°C for 6 h and were quenched by the addition of 5 μl of 5× SDS-PAGE sample

buffer. Samples were separated by SDS-PAGE on 10% gels, and the resulting gels were stained with Coomassie blue. The products were identified by fluorography. Parallel samples were probed by immunoblotting for histone H3 (Abcam 1791).

Chromatin immunoprecipitations (ChIP). Sir2p, Sir4p, and Rap1p binding was analyzed in JPY12 transformed with pDM18 derivatives of histone H3 and H4. Cells were grown to mid-log phase in YEPD medium. Chromatin was immunoprecipitated as described by Kuo and Allis (14) using whole-cell lysate from 1×10^8 cells and 10 μl of polyclonal antibody against Sir2p (Santa Cruz sc-6666), Sir4p (Santa Cruz sc-6671), or Rap1p (M. Grunstein, University of California at Los Angeles; or Santa Cruz sc-20167). The recovered DNA was subjected to semiquantitative, ^{32}P-labeled PCR to determine the relative amount of precipitated DNA. After 25 cycles of amplification, PCR products were electrophoresed on 10% acrylamide, and signals were quantified using a PhosphorImager and ImageQuant v4.2 (Molecular Dynamics). Quantification reflects the amount of precipitated DNA relative to the total input DNA (relative immunoprecipitation [IP]). Each immunoprecipitation was normalized relative to the IP observed for the nonspecific *PHO5* locus. Each experiment was repeated three times, and the data shown are representative of a single experiment. In addition, for each experiment a titration of the input DNA (1:10, 1:50, and 1:100) was included in the PCR quantification to ensure that the PCRs were in the linear range. Primer sets used for PCR quantification are as follows: *HML*α upstream (5′-AGT TTT CGG CAC GGA CTT ATT TGG-3′) and downstream (5′-TAA GAT GCT GCC GCA CAA CTC TC-3′); *HMR***a** upstream (5′-GTC CAA GTT ATG AGC TTA ATC TTC-3′) and downstream (5′-CGG AAT CGA GAA TCT TCG TAA TG-3′); *PHO5* upstream (5′-GAA TCG ATA CAA CCT TGG CAC TC-3′) and downstream (5′-GGT AAT CTC GAA TTT GCT TGC TC-3′). Primer sets for chromosome VI-R have been described previously (21).

Quantitative mating assays. Mating efficiency was assayed in JPY12 transformed with pDM18 derivatives of histone H3 and H4. The mating efficiency of each strain was determined using a quantitative mating assay. Briefly, each mutant strain (*MAT***a**) and the mating-type tester strain CY385 (*MAT*α) were grown to mid-log phase in SC-Trp medium at 37°C. Next, 2×10^6 cells of each mutant strain were mixed with 1×10^7 cells of the tester strain in 5 ml of YEPD medium. Cells were briefly centrifuged and incubated at 30°C for 4 to 7 h. Cells were then resuspended and sonicated gently for 10 s to disrupt clumps, diluted in fresh medium, and plated on SC plates to titer diploid cells and on SC-Lys to titer total cells. The mating efficiency is expressed as the titer of diploid cells divided by the titer of total cells. Data shown are the averages of three experiments with standard errors.

Crystal structure images. SIN and LRS histone mutants were mapped onto the yeast nucleosomal structure (Brookhaven PDB 1ID31) (18) using Pymol (4).

RESULTS

***lrs* mutants do not have a Sin$^-$ phenotype.** The LRS and SIN nucleosomal domains are structurally similar, and alterations in either of these surfaces leads to defects in transcriptional repression. However, despite their loss of silencing phenotypes, *lrs* mutant alleles show no defect in growth either in the presence or absence of wild-type histones, suggesting that their defect is specific to silenced, heterochromatic-like regions of the genome. In contrast, *sin* mutant alleles do affect cell growth and viability when the Sin$^-$ versions are the sole source of histone H3 or H4. H3-E105K, H3-T118I, H3-R116H, and H4-R45C are all inviable as the sole source of histones, whereas H4-V43I and H4-R45H are viable but grow slowly when expressed alone (unpublished results; see also references 16 and 38). Despite the different requirements of intact LRS and SIN domains for yeast cell viability, we wished to test whether each domain contributed to transcriptional silencing by the same mechanism. First, we tested whether *lrs* mutant alleles exhibit a Sin$^-$ phenotype.

In yeast that lack the SWI/SNF chromatin-remodeling complex, an *HO-LacZ* reporter gene is not expressed; however, expression can be partially rescued in the presence of a *sin* mutant histone allele (13, 33). Using this reporter gene, the *lrs* mutant alleles were tested for expression of *HO-LacZ* in an *swi1* mutant that inactivates SWI/SNF. Whereas expression of the H4 R45C *sin* mutant allele led to significant expression of *HO-lacZ* in the *swi1* mutant, expression of several *lrs* mutant alleles had no effect (Fig. 2A and B). As expected, expression of Lrs$^-$ or Sin$^-$ histones had no effect on *HO-lacZ* expression in the presence of an intact SWI/SNF complex (Fig. 2A). Furthermore, expression of Lrs$^-$ histones does not alleviate the slow-growth phenotype of the *swi1* mutant, whereas expression of the H4-R45C or H4-R45H Sin$^-$ version leads to more robust growth on both plates and in liquid media (data not shown). Thus, unlike *sin* mutant alleles, Lrs$^-$ histones do not bypass the SWI/SNF requirement for *HO-lacZ* expression or for wild-type growth rates.

To provide an additional measurement of the Sin$^-$ phenotype, we analyzed expression of *PHO5*. Previously, we showed that *sin* mutant alleles lead to partial derepression of *PHO5* in high-phosphate media, suggesting that the SIN domain contributes to nucleosome-mediated repression of basal transcription (38). To test whether *lrs* mutant alleles have a similar phenotype, *PHO5* expression was monitored by RT-PCR (Fig. 2C). Whereas expression of a *sin* mutant allele (H4-R45C) led to approximately fourfold higher levels of *PHO5* expression, strains containing *lrs* mutant alleles did not significantly derepress *PHO5* (Fig. 2C). These results demonstrate that alterations within the LRS domain do not lead to Sin$^-$ phenotypes in vivo.

The LRS domain is not required for nucleosomal array folding in vitro. Previously we showed that nucleosomal arrays reconstituted with recombinant Sin$^-$ versions of histone H4 are unable to condense into 30-nm-like fibers in vitro (12). To test whether Lrs$^-$ histones also disrupt chromatin folding, we prepared recombinant histone octamers that harbor wild-type histone H3 or an Lrs$^-$ version (H3-R83A), and each of these octamers was used to assemble model nucleosomal arrays (Fig. 3). The previously reported Lrs allele H3-R83A (24) was later shown by resequencing to represent an H3-R83G allele. Therefore, we tested the rDNA-silencing phenotype of H3-R83A for loss of silencing of both rDNA reporters; in fact, H3-R83A displays a similar loss of rDNA silencing to H3-A75V, our control *lrs* mutant allele (Fig. 3D). Our analysis focused on the H3-R83A Lrs$^-$ version, as this arginine residue is structurally equivalent to H4-R45, which is altered in *sin* mutant alleles (Fig. 1). A DNA template composed of 11 copies of a 208-bp 5S rRNA gene isolated from the sea urchin *Lytechinus variegatus* (the 208-11 template) was used to generate a positioned array of 11 nucleosomes after in vitro salt dialysis reconstitution (5). As observed previously for Sin$^-$ histones (12), the Lrs$^-$ version of H3 had no effect on histone octamer assembly (data not shown).

The folding of nucleosomal arrays into 30-nm-like fibers in vitro requires that arrays be fully saturated with nucleosomes (e.g., 11 nucleosomes per array) (29). As an initial means of monitoring the efficiency of nucleosomal array assembly, we digested the reconstituted arrays with EcoRI. Because each 5S ribosomal DNA repeat in the 208-11 array template is bordered by EcoRI restriction sites, EcoRI cleavage releases either a 208-bp free DNA fragment or a mononucleosome that can be identified by its slower mobility after native gel electrophoresis. A fully saturated nucleosomal array typically yields

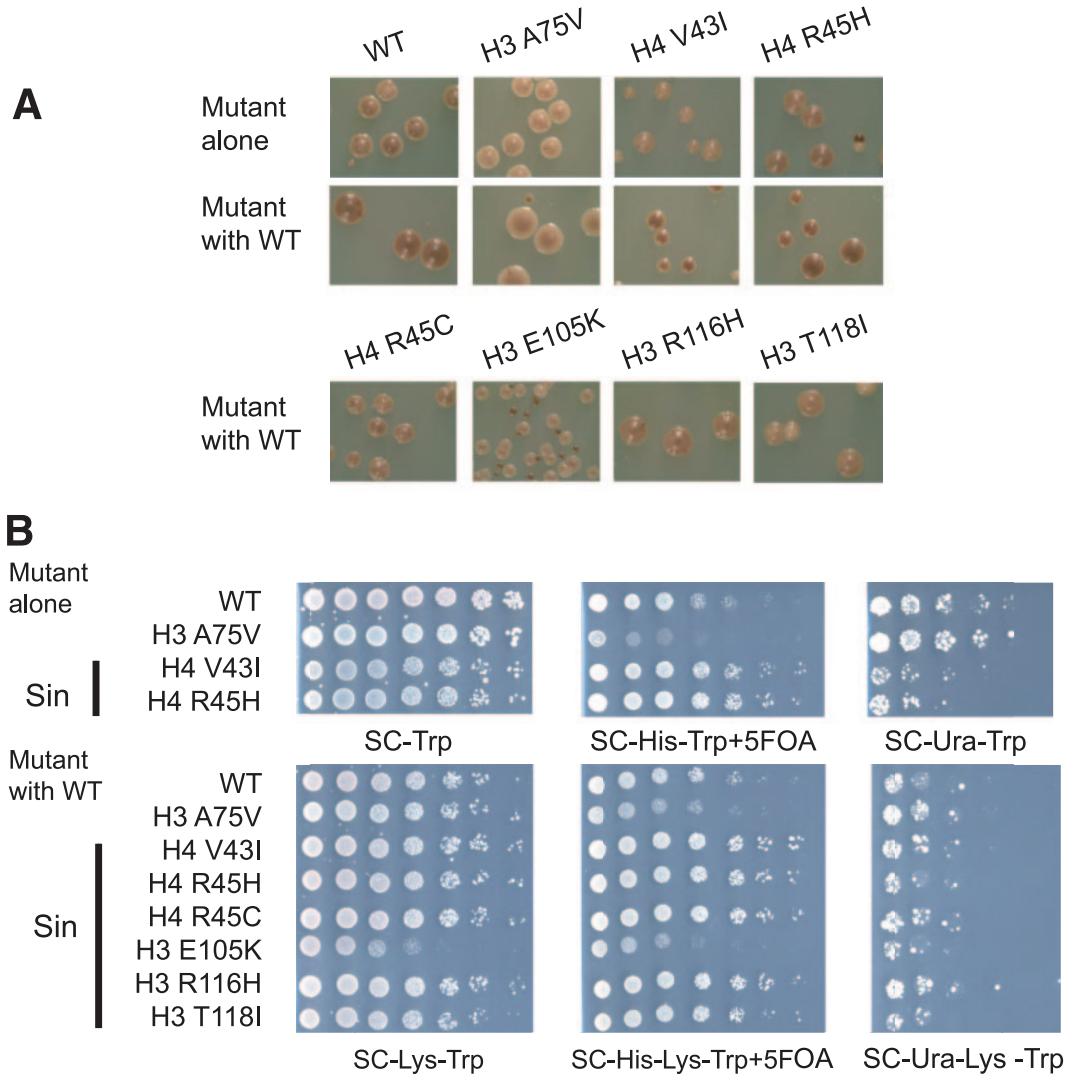

FIG. 4. Sin$^-$ alterations do not disrupt ribosomal DNA silencing. Silencing was measured by assaying for expression of two RNA polymerase II-transcribed reporter genes: (A) the *MET15* reporter inserted in the *NTS2* region and (B) the *mURA3* reporter in the 5′ region of the 35S rRNA gene. Mutant with wild-type designates the JPY12 strain containing a wild-type *HHT1-HHF1* pJP11 plasmid and the indicated wild-type (WT) or mutant histone *HHT2-HHF2* pDM18 plasmid (Lys$^+$ Trp$^+$ cells). Mutant alone designates the JPY12 strain containing only the mutant histone pDM18 plasmid (Lys$^-$ Trp$^+$ cells). Control strains include the wild type (WT) containing one or two wild-type histone plasmids and the histone H3 Lrs$^-$ mutant A75V.

~2 to 5% free DNA in this EcoRI assay (2). Recombinant wild-type and Lrs$^-$ histone octamers yielded similar levels of nucleosome density at nearly identical ratios of octamers to the 5S ribosomal DNA repeat (ratios of 1.0 to 1.4), indicating that the Lrs$^-$ version of H4 does not disrupt nucleosome assembly (Fig. 3A).

In low-ionic-strength buffers, such as Tris-EDTA (TE), 208-11 arrays exist as extended, flexible fibers that sediment in the analytical ultracentrifuge as a nearly homogeneous distribution of ~27S-28S species (17, 29). Previously we showed that arrays reconstituted with Sin$^-$ histones sediment slightly slower in TE buffer compared to wild-type arrays, and this observation led us to suggest that Sin$^-$ arrays may be more extended in low-salt conditions (12). In contrast, the sedimentation of the Lrs$^-$ nucleosomal arrays was identical to that of a wild-type array (Fig. 3B, open symbols).

When divalent cations (Mg^{2+}) are introduced, these model nucleosomal arrays form a heterogeneous, faster-sedimenting species with a 30S-55S distribution (Fig. 3B) (29); formation of the 55S species is consistent with formation of a compact, 30-nm-like chromatin fiber. Saturated Sin$^-$ nucleosomal arrays sediment at only ~30S in Mg^{2+}-containing buffer, reflecting a complete absence of salt-dependent folding (12). In contrast to the Sin$^-$ arrays, nucleosomal arrays reconstituted with the H3-R83A Lrs$^-$ histone are fully competent for formation of compact, 30-nm-like fibers exhibiting a typical 30S-55S distribution (Fig. 3B, closed circles).

In addition to these intramolecular folding reactions, higher concentrations of divalent cations can induce reversible oligomerization of nucleosomal arrays (28). Intermolecular oligomerization generates large (>1,000S), defined structures that are believed to mimic the fiber-fiber interactions that stabilize

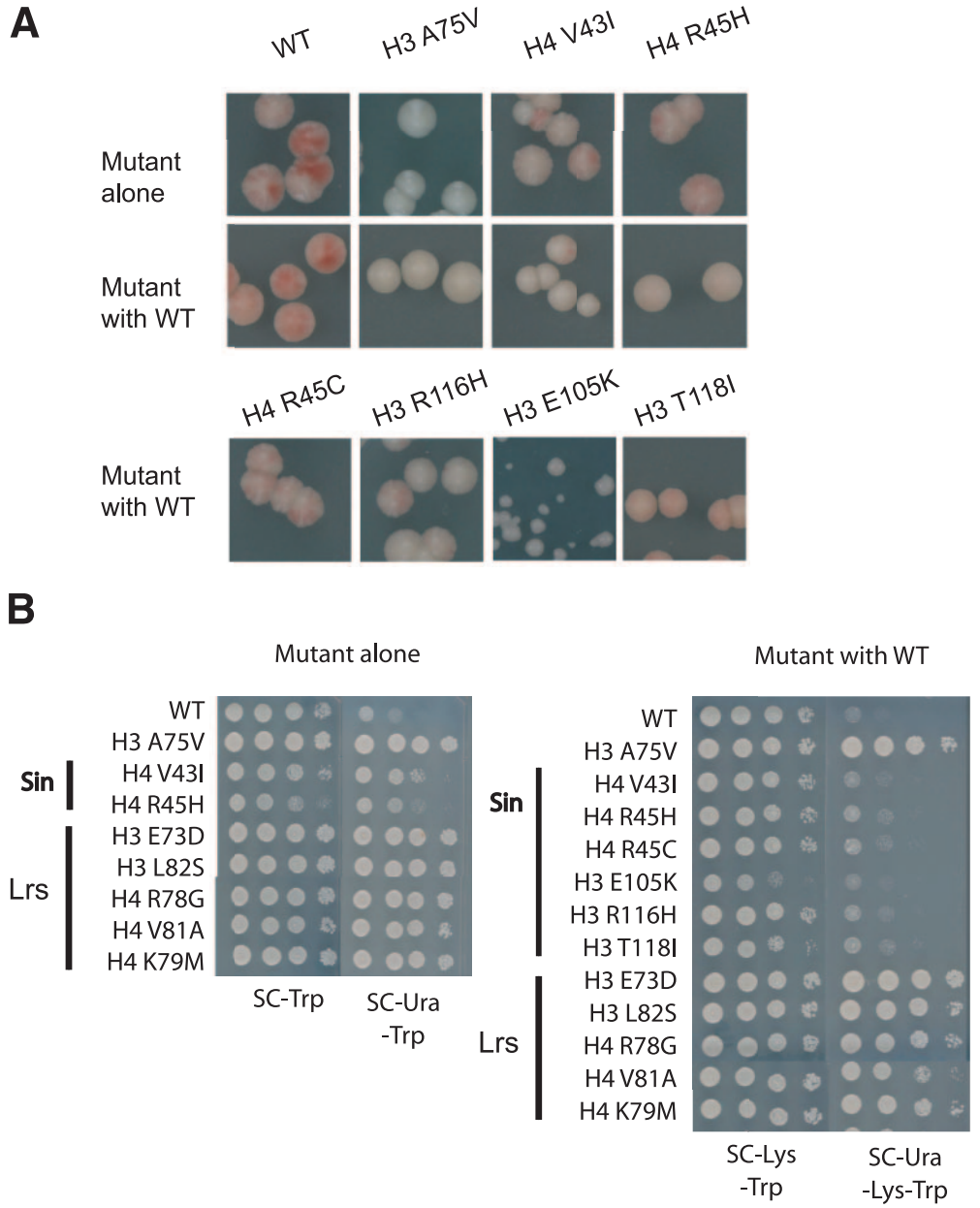

FIG. 5. Both Lrs$^-$ and Sin$^-$ alterations disrupt telomeric silencing. Silencing was measured in strain ANY34 by assaying for expression of two reporter genes: (A) the *ADE2* reporter gene integrated at the *V-R* telomere and (B) the *URA3* reporter gene integrated at the *VII-L* telomere. Mutant with wild type designates the ANY34 strain containing a wild-type *HHT1-HHF1* pJP11 plasmid and the indicated wild-type (WT) or mutant histone *HHT2-HHF2* pDM18 plasmid (Lys$^+$ Trp$^+$ cells). Mutant alone designates the ANY34 strain containing only the mutant histone pDM18 plasmid (Lys$^-$ Trp$^+$ cells). Control strains include the wild type (WT) containing one or two wild-type histone plasmids and the histone H3 Lrs$^-$ mutant A75V, which displays loss of telomeric silencing.

higher order chromosomal domains. Sin$^-$ histones do not disrupt the oligomerization of model 5S nucleosomal arrays (12), and likewise the Lrs$^-$ version, H4-R83A, has no effect on formation of these higher order structures (Fig. 3C). Thus, even though Lrs$^-$ and Sin$^-$ nucleosomes have lost a similar number of histone-DNA contacts, only Sin$^-$ histones selectively disrupt the intramolecular folding of nucleosomal arrays in vitro.

Sin$^-$ mutants do not have a loss of ribosomal DNA-silencing (LRS) phenotype. Although *lrs* mutant alleles do not show Sin$^-$ phenotypes in vivo or in vitro, we also investigated whether *sin* mutant alleles show an Lrs$^-$ phenotype. *lrs* mutant alleles were identified using two RNA polymerase II-transcribed reporter genes inserted within the ribosomal DNA locus, the *MET15* reporter in the NTS2 region, and the *mURA3* reporter (with a minimal *TRP1* promoter) in the 5′ region of the 35S rRNA gene (24). The *lrs* mutant alleles lead to a loss of ribosomal DNA silencing, meaning that strains harboring these mutant histones do not grow well on 5-FOA media, reflecting a loss of silencing of *URA3*, and similarly the

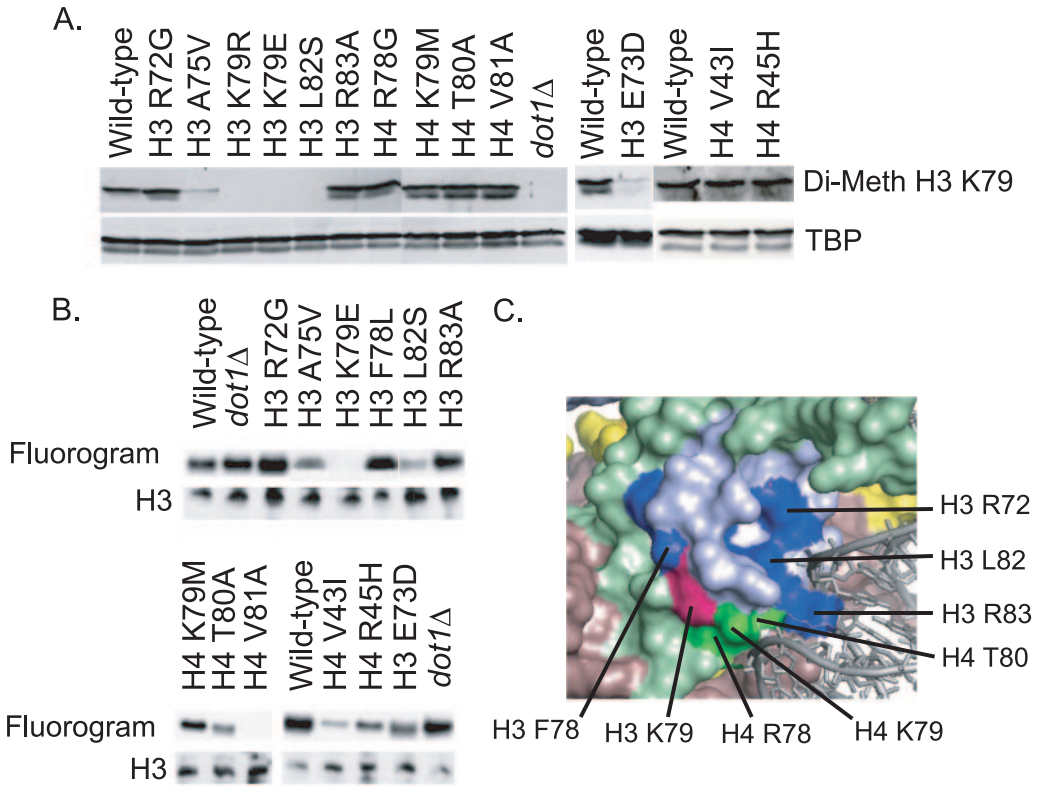

FIG. 6. Sin$^-$ and Lrs$^-$ alterations do not generally disrupt H3-K79 methylation. (A) JPY12 cells expressing either wild-type, Lrs$^-$, or Sin$^-$ histones as the sole source of histone H3 or H4 were grown to mid-log phase in YEPD medium. Cells were lysed in Laemmli buffer and lysates were analyzed by SDS-PAGE, followed by Western blot analysis with antibodies raised against histone H3 dimethyl K79 and TBP (loading control; upper panel) or histone H3 trimethyl K79 and total histone H3 (loading control; lower panel). (B) Soluble chromatin was isolated from wild-type (JPY12), *dot1*Δ (EMHY234), and a series of *dot1*Δ Lrs$^-$ strains and incubated with recombinant Dot1p and [^{3}H]*S*-adenosyl-methionine. Reaction products were separated by SDS-PAGE, and methylated histone H3 was detected by fluorography (upper panel). Histone H3 was detected by immunoblot analysis to normalize input levels of histone proteins in each reaction (lower panel).

colonies display a lighter tan color, in contrast to wild-type colonies on MLA (lead) plates due to loss of *MET15* silencing. We tested the ability of *sin* mutants to form repressive chromatin at the ribosomal DNA using the above-mentioned reporter system. The viable H4 *sin* mutant alleles, V43I and R45H, display a slight increase in ribosomal DNA silencing, giving a slightly darker color than the wild type on lead plates and showing enhanced growth on 5-FOA as measured by serial dilution (Fig. 4). Similarly, the inviable *sin* mutant alleles, H4-R45C, H3-T118I, H3-E105K, and H3-R116H, display wild-type ribosomal DNA-silencing phenotypes. H3-E105K displays a dominant slow-growth phenotype and hence displays smaller colonies overall. The small, darker colonies present on the MLA plates are due to loss of the *MET15* reporter by recombination. The same small-colony phenotype is also observed in the telomeric silencing reporter strains (Fig. 5). In contrast, the control *lrs* mutants are a lighter color compared to the wild-type strain on lead-containing plates (Fig. 4A) and grow less well compared to the wild type on plates that contain 5-FOA (Fig. 4B). Thus, disruption of the SIN domain does not lead to an Lrs$^-$ phenotype, reinforcing the view that the SIN and LRS nucleosomal surfaces are functionally distinct.

Alterations in both the SIN and LRS domains disrupt telomeric silencing. The LRS surface is also important for both telomeric and, to a lesser extent, silent mating-type locus silencing (24). Although alterations of the SIN surface do not display a loss of ribosomal DNA silencing, it is possible that they could share other silencing defects. The mechanism of ribosomal DNA silencing differs from that of telomeric or HM silencing in that *SIR3* and *SIR4* are not required. Also, the ribosomal DNA, while inhibitory to Pol II transcription, is very active in Pol I and Pol III transcription, indicating that some components of the mechanisms of silencing for the ribosomal DNA are distinct (1, 3, 27). The *sin* mutant alleles were tested for telomeric silencing defects using subtelomeric *URA3* and *ADE2* reporters. In wild-type yeast, the majority of such cells repress subtelomeric reporters, thereby permitting cells to grow on 5-FOA and displaying red or pink colonies with white sectors (10). However, cells defective in telomeric silencing express *URA3* and are sensitive to 5-FOA, and colonies have a white or light pink color when grown on nonselective media with limiting adenine. Both *sin* and *lrs* mutant alleles display defects in telomeric silencing (Fig. 5). In the presence of wild-type histones, only one of the H3 *sin* mutant alleles showed a strong defect in telomeric silencing. In contrast, the H4 *sin* mutant alleles showed a strong silencing defect when the Sin$^-$ histones were expressed as the sole source of H4. The *lrs* mutant alleles, with the exception of H3-K79R, also show a

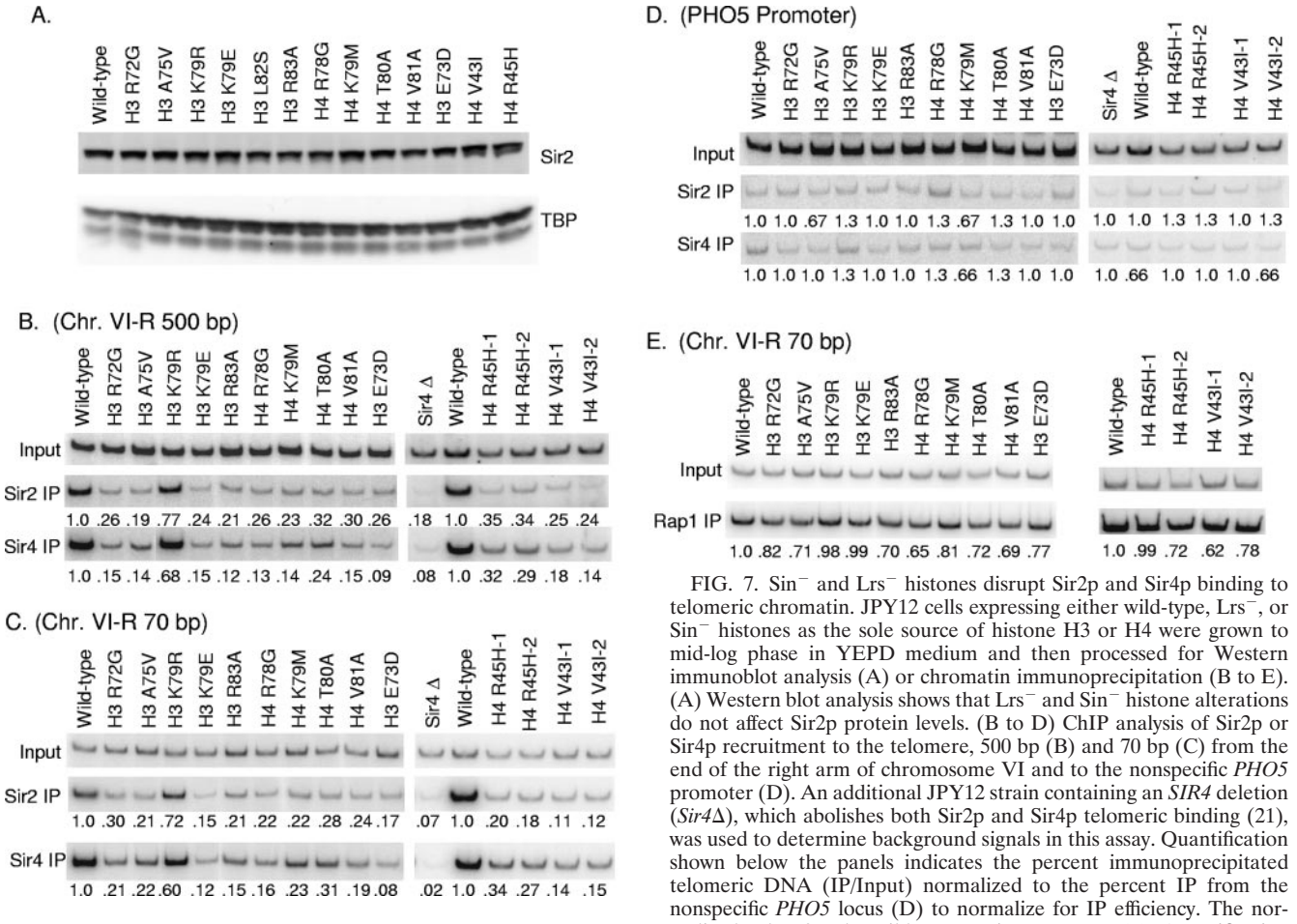

FIG. 7. Sin$^-$ and Lrs$^-$ histones disrupt Sir2p and Sir4p binding to telomeric chromatin. JPY12 cells expressing either wild-type, Lrs$^-$, or Sin$^-$ histones as the sole source of histone H3 or H4 were grown to mid-log phase in YEPD medium and then processed for Western immunoblot analysis (A) or chromatin immunoprecipitation (B to E). (A) Western blot analysis shows that Lrs$^-$ and Sin$^-$ histone alterations do not affect Sir2p protein levels. (B to D) ChIP analysis of Sir2p or Sir4p recruitment to the telomere, 500 bp (B) and 70 bp (C) from the end of the right arm of chromosome VI and to the nonspecific *PHO5* promoter (D). An additional JPY12 strain containing an *SIR4* deletion (*Sir4*Δ), which abolishes both Sir2p and Sir4p telomeric binding (21), was used to determine background signals in this assay. Quantification shown below the panels indicates the percent immunoprecipitated telomeric DNA (IP/Input) normalized to the percent IP from the nonspecific *PHO5* locus (D) to normalize for IP efficiency. The normalized value for the wild-type strain was set at 1.0. Quantification below panel D indicates the percent immunoprecipitated *PHO5* DNA (IP/Input), with the value for wild-type cells set at 1.0. (E) Rap1p binding 70 bp from the end of the right arm of chromosome VI was analyzed using antibodies to Rap1p. Similar results were observed in an independent experiment. Chr., chromosome.

loss of telomeric silencing (Fig. 5; see also reference 24). Thus, the SIN and LRS domains are both required for telomeric gene silencing.

The SIN and LRS domains are not generally required for H3-K79 methylation. A current view is that methylation of H3-K79 distinguishes euchromatin from heterochromatin by preventing Sir protein association in euchromatic regions (37). Inactivation of Dot1p, the H3-K79 methylase, is thought to cause Sir proteins to delocalize from the silenced regions and redistribute throughout the genome (37), leading to a disruption of silencing. Given that H3-K79 is within the LRS domain, we tested the simple hypothesis that *lrs* mutant alleles disrupt silencing because they cripple the binding or activity of the Dot1p methylase. Likewise, it is also a formal possibility that the SIN domain is required for Dot1p function. First, we used Western blot analysis to monitor the levels of H3-K79 di- and trimethylation in bulk chromatin from cells that express wild-type, Lrs$^-$, or Sin$^-$ histones as the sole source of histone protein. Figure 6 demonstrates that most *lrs* mutant alleles are not defective in H3-K79 di- or trimethylation, ruling out the hypothesis that their only role in controlling silencing is mediated through Dot1p binding. Likewise, the H4 Sin$^-$ versions do not disrupt H3-K79 di- or trimethylation as measured by immunoblotting in vivo (Fig. 6A).

As an additional test for whether *lrs* mutant alleles disrupt Dot1p function, we also performed in vitro labeling analyses. Soluble chromatin was isolated from *dot1*Δ cells harboring either wild-type or Lrs$^-$ histones and incubated with recombinant Dot1p and radioactive *S*-adenosyl-methionine. Reaction products were separated by SDS-PAGE, and methylated histone H3 was detected by fluorography. Consistent with the bulk chromatin analysis, only a small subset of *lrs* mutant alleles eliminated Dot1p-dependent methylation (Fig. 6B). The results agree with the immunoblotting results, except that one mutant that was immunoreactive in vivo did not show in vitro labeling for unknown reasons (V81A). Overall, these results are consistent with previous reports showing that an H3-K79A substitution has a more severe effect on Sir protein occupancy of silenced regions than loss of Dot1p (23, 37). These data support the view that the SIN and LRS domains do not function solely by influencing Dot1p binding or by controlling methylation of H3-K79.

LRS and SIN domains are required for Sir2p and Sir4p binding to telomeric chromatin. To further investigate the role of the LRS and SIN domains in telomeric silencing, we mon-

TABLE 2. LRS and SIN domains function with Sir1p to silence *HM* loci[a]

Strain	Description	% Mating efficiency
JPY12	H3 WT	100
CY1109	H3 WT *sir1*Δ	4.4 ± 0.9
CY1113	H3 WT *sir4*Δ	<0.5
CY1045	H3-K79E	<0.5
CY1110	H3-K79E *sir1*Δ	<0.5
CY1044	H3-K79R	94.0 ± 8.9
CY1111	H3-K79R *sir1*Δ	<0.5
CY1047	H3-R83A	68.2 ± 2.5
CY1112	H3-R83A *sir1*Δ	<0.5
CY1169	H4-R45H	28.2 ± 6.2
CY1278	H4-R45H *sir1*Δ	<0.5
CY1171	H4-V43I	75.6 ± 4.5
CY1279	H4-V43I *sir1*Δ	<0.5

[a] WT, wild type. Mating efficiency was normalized to the H3 WT strain (set at 100%).

itored recruitment of two components of the silencing machinery, Sir2p and Sir4p, by chromatin immunoprecipitation analysis. In wild-type cells, Sir2p and Sir4p were formaldehyde cross-linked to chromatin at 70 bp and 500 bp distal to telomere VIR (Fig. 7B and C). In the absence of Sir4p, recruitment of Sir2p was reduced to 18% (500 bp) or 7% (70 bp) of wild-type levels, and the signal for the Sir4p immunoprecipitations was reduced to 8% (500 bp) or 2% (70 bp) of the wild type. These values reflect background signals in these studies, so the actual fold reductions in binding may be significantly higher. Strikingly, in cells that express *lrs* mutant alleles or viable *sin* mutant alleles (H4-R45H and H4-V43I), Sir2p and Sir4p recruitment at both the 500-bp and 70-bp regions was reduced at least sixfold in most cases (Fig. 7B and C). In contrast, recruitment of Rap1p to the end of the telomere was unaffected by Lrs$^-$ or Sin$^-$ histones (Fig. 7E). Importantly, Lrs$^-$ and Sin$^-$ alterations do not affect cellular levels of Sir2p or Sir4p as assayed by Western blot (Fig. 7A and data not shown). In general, the defects in telomere recruitment of

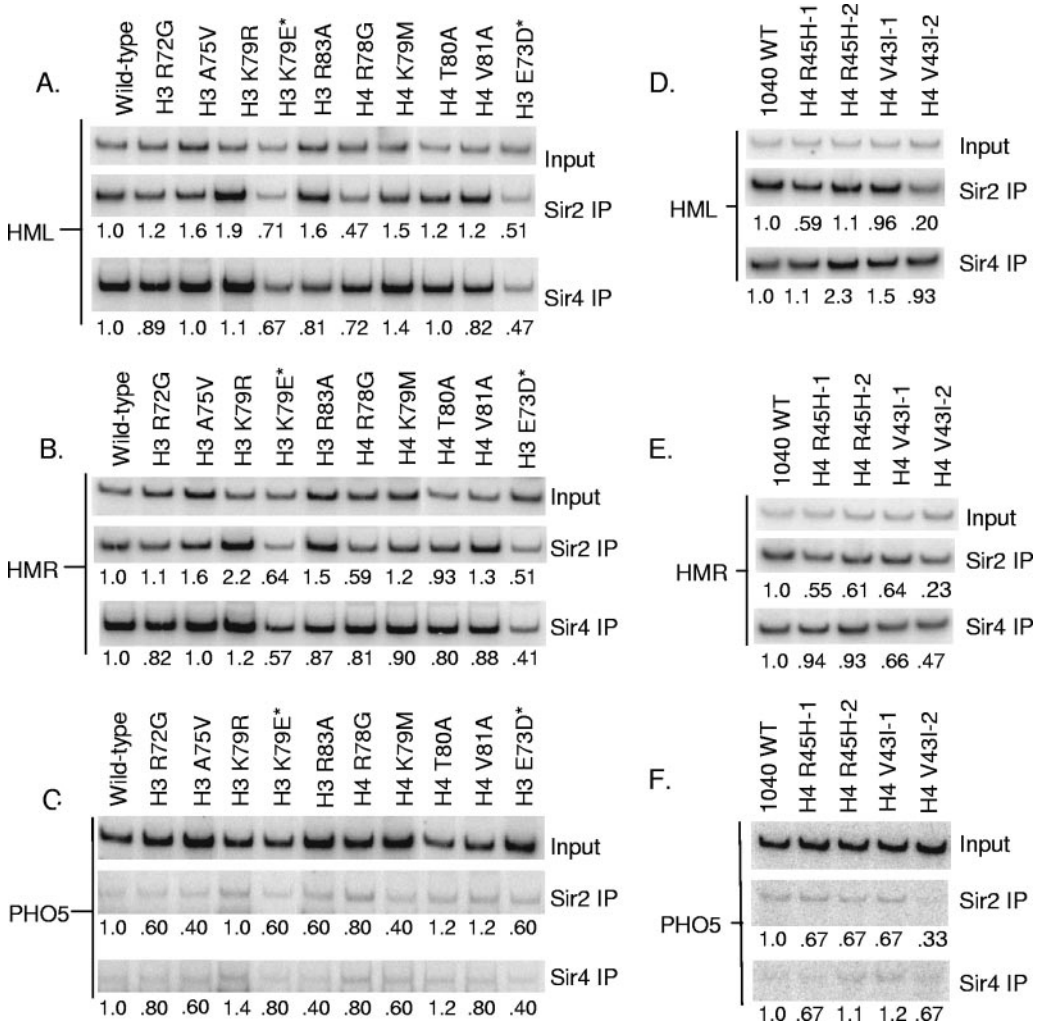

FIG. 8. Sin$^-$ and Lrs$^-$ histones do not disrupt Sir2p and Sir4p binding to silent *HML* and *HMR* chromatin. Binding of Sir2p and Sir4p to the silent mating-type loci *HML* and *HMR* and the nonspecific *PHO5* promoter in JPY12 cells harboring either wild-type, Lrs$^-$ (A to C), or Sin$^-$ (D to F) histones as the sole source of histone H3 or H4 was examined using ChIP analysis, as described in the legend to Fig. 7. An asterisk designates mutations that have previously been shown to disrupt mating (24, 35).

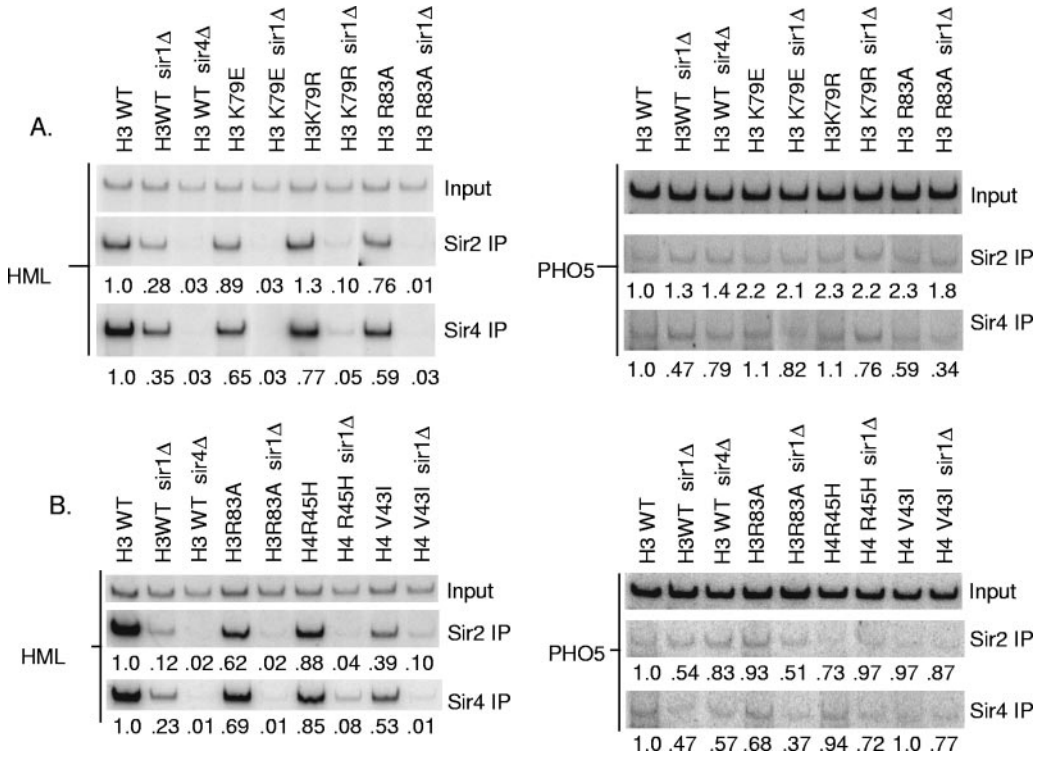

FIG. 9. In the absence of Sir1p, Sin$^-$ and Lrs$^-$ histones abolish Sir2p and Sir4p binding to silent *HML* chromatin. (A) JPY12 cells containing the indicated *SIR* gene deletions and harboring either wild-type, Lrs$^-$, or Sin$^-$ histones as the sole source of histone H3 or H4 were grown to mid-log phase in YEPD medium and processed for ChIP analysis, as described in the legend to Fig. 7. (A) Binding of Sir2p and Sir4p to *HML* in strains containing histone H3 Lrs$^-$ alterations compared to strains containing wild-type histone H3. (B) Binding of Sir2p and Sir4p to *HML* in strains containing Sin$^-$ histone alterations compared to wild-type histone H3 and the H3 R83A Lrs$^-$ alteration. As a control for nonspecific binding, Sir2p and Sir4p binding to the *PHO5* promoter is also shown. Sir2p and Sir4p binding to *HML* was normalized to the amount of binding observed for the nonspecific *PHO5* locus as described in the legend to Fig. 7. WT, wild type.

Sir2p or Sir4p closely parallel the observed defects in telomeric silencing.

LRS and SIN domains function with Sir1p to recruit Sir2p and Sir4p to HM chromatin. An intact LRS domain is required for full silencing of an RNA polymerase II reporter gene that is inserted within the *HML* silent mating type locus (24). However, except for H3-K79E and H3-L82S, most *lrs* mutant alleles do not appear to strongly derepress the native *HM* loci, as the mutants mate normally and show wild-type levels of Sir2p and Sir4p recruitment to the *HML* and *HMR* loci (Table 2; Fig. 8A and B) (24). Likewise, alterations within the SIN domain do not lead to dramatic defects in mating or Sir protein recruitment to *HM* loci, although the H4-R45H allele does show a reproducible defect in these assays (Table 2; Fig. 8D and E). Why should the LRS and SIN domains be required for Sir protein recruitment at telomeres but not at *HM* loci? A major difference between telomeric and *HM* silencing is that Sir1p is required specifically at the *HM* loci for the recruitment and stabilization of Sir2p, Sir3p, and Sir4p (25, 31). If the LRS and SIN domains provide an additional binding surface for assembly of Sir proteins on chromatin, we entertained the possibility that Sir1p might play a partially redundant role with these nucleosomal surfaces. To test this hypothesis, we monitored mating and Sir protein recruitment in *sir1*Δ strains that harbored wild-type, Lrs$^-$, or Sin$^-$ histones.

In the absence of Sir1p, both the LRS and SIN domains are essential for mating and for Sir2p and Sir4p recruitment. In an *sir1*Δ strain, cells mate at ~4.5% efficiency when wild-type histones are present, but expression of Lrs$^-$ or Sin$^-$ histones cripples mating to undetectable levels (Table 2). Likewise, in the absence of Sir1p, recruitment of Sir2p and Sir4p is reduced approximately three- to fivefold in the strain that expresses wild-type histones (Fig. 9), but in both *lrs* and *sin* mutants, recruitment of Sir2p and Sir4p is reduced to background levels (Fig. 9) that parallel the defects found at the telomere (Fig. 8). Thus, the LRS and SIN domains are required for optimal Sir2p and Sir4p binding at both telomeric and *HM* loci, and in the case of the *HM* loci this role is partially redundant with Sir1p function.

Given that Sir2p is the only common factor required for all three forms (*HM*, telomeres, and ribosomal DNA) of silencing in yeast, a phenotype it shares with the LRS domain, it is tempting to hypothesize that the LRS surface is an Sir2p binding site. If this is the case, one would expect that overexpression of *SIR2* would selectively relieve the ribosomal DNA-silencing defects of the *lrs* mutants. In fact, we find that overexpression of Sir2p increases ribosomal DNA silencing in all strains, including the wild type (Fig. 10). In support of general silencing enhancement by Sir2p, overexpression of *SIR4*, which is known to deplete Sir2p from the ribosomal DNA and increase recruitment to telomeres in wild-type cells (32), exacerbates the ribosomal DNA-silencing defects of both

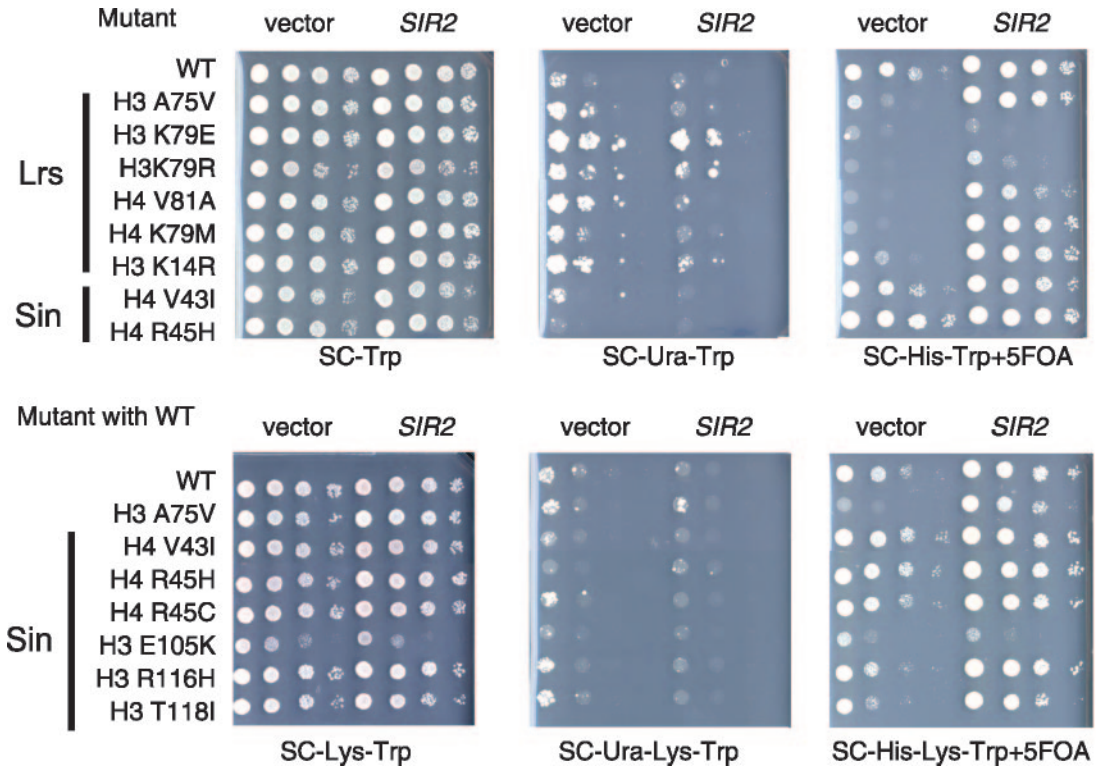

FIG. 10. Sir2 overexpression does not rescue the ribosomal DNA-silencing phenotype of *lrs* or *sin* mutant alleles. JPY12 strains harboring both *sin* and *lrs* mutant alleles were transformed with a 2-μm vector containing *SIR2* or an empty vector, and silencing of the *mURA3* reporter gene inserted in the 5′ region of the 35S rRNA gene was assayed by measuring growth on SC-Ura and SC-His plus 0.1% 5-FOA. Mutant with wild type designates the ANY34 strain containing a wild-type *HHT1-HHF1* pJP11 plasmid and the indicated wild-type (WT) or mutant histone *HHT2-HHF2* pDM18 plasmid (Lys^+ Trp^+ cells). Mutant alone designates the ANY34 strain containing only the mutant histone pDM18 plasmid (Lys^- Trp^+ cells).

the *lrs* and *sin* mutants equally (Fig. 10). Additionally, the telomeric silencing defect shared by *sin* and *lrs* mutants is only slightly reduced by overexpression of *SIR2*.

DISCUSSION

The *sin* and *lrs* mutant alleles of histone genes were both identified in unbiased screens for specific phenotypes, and no overlap was seen between the two collections of alleles (13, 24). However, in both cases, the mutations alter a cluster of amino acid residues that define two structurally similar DNA-histone contact surfaces. Thus, it seemed likely that loss of the DNA-histone contact at SHL ±2.5 (*lrs* mutant alleles) or loss of contact at SHL ±0.5 (*sin* mutant alleles) might yield similar changes in chromatin structure in vitro and in vivo. However, we found that *lrs* mutants do not show a Sin^- phenotype in vivo, nor do *sin* mutants show loss of ribosomal DNA silencing. In vitro these two nucleosomal surfaces also show distinct properties. Although both Sin^- and Lrs^- histones are fully competent for assembly of nucleosomes, only Sin^- nucleosomes disrupt the salt-dependent formation of compact, 30-nm-like fibers (12). This disparity suggests that unlike the SIN surface, the LRS surface is not important for formation of this particular higher order chromatin structure. This latter observation also illustrates that loss of a single DNA-histone contact does not lead to an obligatory defect in chromatin folding. Our study reinforces the view that each histone-DNA contact site is functionally distinct and, moreover, that the nucleosome can be divided into distinct surfaces that exert different functions.

The SIN and LRS surfaces are required for telomeric and *HM* silencing. Although only *lrs* mutants disrupt gene silencing at the ribosomal DNA locus, both the SIN and LRS domains are required for silencing of a reporter gene that is integrated close to a telomere. Furthermore, amino acid substitutions within either the SIN or LRS domain disrupted the binding of Sir2p and Sir4p at telomeric chromatin. Additionally, both LRS and SIN surfaces are important for *HM* loci silencing and Sir2p and Sir4p binding to *HM* chromatin. Their defects are decidedly less dramatic at the *HM* loci relative to telomeres, potentially reflecting the redundancy of factors responsible for recruiting the Sir2/Sir3/Sir4 complex to the *HM* loci (25). The synergistic effect of an *sir1*Δ and both *lrs* and *sin* mutant alleles in both *HM* loci silencing and binding of Sir2p and Sir4p suggests that both nucleosomal surfaces participate in pathways parallel to *SIR1* and upstream of Sir2/Sir3/Sir4 recruitment to the *HM* loci.

These two nucleosomal surfaces highlight the differences and similarities between the two types of silenced regions of the genome, namely ribosomal DNA and telomeric/*HM* loci. Telomeric and *HM* silencing share similar requirements for *trans*-acting factors, namely Sir2, Sir3, Sir4, and Rap1. *HM* silencing also requires Sir1p. In contrast, ribosomal DNA si-

lencing does not require the *trans*-acting Sir1p, Sir3p, or Sir4p but instead depends on Sir2p and other subunits of the RENT complex (34). These different protein requirements may reflect a fundamental difference between ribosomal DNA silencing and the other two forms of silencing (26). While the differences are many, the commonalities are the absolute requirement for Sir2p and the LRS surface.

There are at least three ways that Sin$^-$ or Lrs$^-$ histone might disrupt heterochromatin formation: (i) there can be defects in the ability to organize the DNA, (ii) there can be defects in the ability to associate with other nucleosomes, or (iii) there can be defects in the ability to associate with a *trans*-acting factor. An Lrs$^-$ version of histone H3 is fully competent to organize DNA into nucleosomes in vitro, and arrays of these Lrs$^-$ nucleosomes can undergo normal salt-dependent condensation. These observations argue against models (i) and (ii) and suggest the possibility that the LRS surface may interact with a key *trans*-acting factor that influences Sir2p binding. While it is tempting to hypothesize that the LRS surface is an Sir2p binding site, overexpression of Sir2p does not specifically alleviate the ribosomal DNA-silencing phenotype of *lrs* mutant alleles, and little suppression is seen for the telomeric silencing phenotype. Additionally, *lrs* mutant alleles display only small defects in *HM* loci silencing despite an absolute requirement for Sir2p. Although the lack of a specific effect of *SIR2* overexpression on LRS mutants is not unequivocal, it does suggest that there might be some other factor that binds to the LRS surface which itself influences or directly promotes Sir2p binding.

Although *sin* mutant alleles alter key histone-DNA contacts at the nucleosomal dyad, Sin$^-$ histone octamers organize DNA into nucleosomes that are nearly identical in structure to canonical nucleosomes (22). Sin$^-$ mononucleosomes do show an enhanced propensity to slide along DNA in *cis* at lower temperatures than wild-type mononucleosomes (33 to 42° versus 43°C) (7, 22), although Sin$^-$ nucleosomal arrays do not show changes in nucleosome positioning or DNA accessibility even after extended incubation at 37°C (12). What is quite clear is that Sin$^-$ nucleosomal arrays are unable to condense into 30-nm-like fibers in vitro (12). Thus, a simple model for the role of the SIN domain in silencing proposes that the optimal substrate for Sir2/Sir3/Sir4, but perhaps not the RENT complex, is a folded nucleosomal array. The RENT complex may be competent to bind nucleosomes in or out of the context of higher order chromatin. Alternatively, an ordered, compact structure may not be required for ribosomal DNA silencing as it is for both telomeric and *HM* loci silencing. In conclusion, our study reinforces the view that although the nucleosome is one complex made up of several histone fold motifs, it has functionally distinct surfaces that exert unique functions.

ACKNOWLEDGMENTS

We thank Kimberly Crowley for help with the sedimentation velocity studies and Peter Horn for XL-I data analysis, Edel Hyland for strains, and Fred van Leeuwen and Dan Gottschling for information and Dot1 reagents prior to publication.

This work was supported by a postdoctoral fellowship from the Leukemia and Lymphoma Society of America to C.J.F., a grant from the NIH (GM54096) to C.L.P., and a grant from the NIH (GM62385) to J.D.B.

REFERENCES

1. **Buck, S. W., J. J. Sandmeier, and J. S. Smith.** 2002. RNA polymerase I propagates unidirectional spreading of rDNA silent chromatin. Cell **111:** 1003–1014.
2. **Carruthers, L. M., C. Tse, K. P. Walker III, and J. C. Hansen.** 1999. Assembly of defined nucleosomal and chromatin arrays from pure components. Methods Enzymol. **304:**19–35.
3. **Cioci, F., L. Vu, K. Eliason, M. Oakes, I. N. Siddiqi, and M. Nomura.** 2003. Silencing in yeast rDNA chromatin: reciprocal relationship in gene expression between RNA polymerase I and II. Mol. Cell **12:**135–145.
4. **DeLano, W. L.** 2002. The PyMOL molecular graphics system. Delano Scientific, San Carlos, Calif.
5. **Dong, F., J. C. Hansen, and K. E. van Holde.** 1990. DNA and protein determinants of nucleosome positioning on sea urchin 5S rRNA gene sequences in vitro. Proc. Natl. Acad. Sci. USA **87:**5724–5728.
6. **Duina, A. A., and F. Winston.** 2004. Analysis of a mutant histone H3 that perturbs the association of Swi/Snf with chromatin. Mol. Cell. Biol. **24:**561–572.
7. **Flaus, A., C. Rencurel, H. Ferreira, N. Wiechens, and T. Owen-Hughes.** 2004. Sin mutations alter inherent nucleosome mobility. EMBO J. **23:**343–353.
8. **Fletcher, T. M., and J. C. Hansen.** 1995. Core histone tail domains mediate oligonucleosome folding and nucleosomal DNA organization through distinct molecular mechanisms. J. Biol. Chem. **270:**25359–25362.
9. **Goldstein, A. L., and J. H. McCusker.** 1999. Three new dominant drug resistance cassettes for gene disruption in Saccharomyces cerevisiae. Yeast **15:**1541–1553.
10. **Gottschling, D. E., O. M. Aparicio, B. L. Billington, and V. A. Zakian.** 1990. Position effect at S. cerevisiae telomeres: reversible repression of Pol II transcription. Cell **63:**751–762.
11. **Hansen, J. C., J. Ausio, V. H. Stanik, and K. E. van Holde.** 1989. Homogeneous reconstituted oligonucleosomes, evidence for salt-dependent folding in the absence of histone H1. Biochemistry **28:**9129–9136.
12. **Horn, P. J., K. Crowley, L. M. Carruthers, J. C. Hansen, and C. L. Peterson.** 2002. The SIN domain of the histone octamer is essential for intramolecular folding of nucleosomal arrays. Nat. Struct. Biol. **9:**167–171.
13. **Kruger, W., C. L. Peterson, A. Sil, C. Coburn, G. Arents, E. N. Moudrianakis, and I. Herskowitz.** 1995. Amino acid substitutions in the structured domains of histones H3 and H4 partially relieve the requirement of the yeast SWI/SNF complex for transcription. Genes Dev. **9:**2770–2779.
14. **Kuo, M. H., and C. D. Allis.** 1999. In vivo cross-linking and immunoprecipitation for studying dynamic protein:DNA associations in a chromatin environment. Methods **19:**425–433.
15. **Kurumizaka, H., and A. P. Wolffe.** 1997. Sin mutations of histone H3: influence on nucleosome core structure and function. Mol. Cell. Biol. **17:** 6953–6969.
16. **Lenfant, F., R. K. Mann, B. Thomsen, X. Ling, and M. Grunstein.** 1996. All four core histone N-termini contain sequences required for the repression of basal transcription in yeast. EMBO J. **15:**3974–3985.
17. **Logie, C., and C. L. Peterson.** 1997. Catalytic activity of the yeast SWI/SNF complex on reconstituted nucleosome arrays. EMBO J. **16:**6772–6782.
18. **Luger, K., A. W. Mader, R. K. Richmond, D. F. Sargent, and T. J. Richmond.** 1997. Crystal structure of the nucleosome core particle at 2.8 A resolution. Nature **389:**251–260.
19. **Luger, K., T. J. Rechsteiner, and T. J. Richmond.** 1999. Expression and purification of recombinant histones and nucleosome reconstitution. Methods Mol. Biol. **119:**1–16.
20. **Luger, K., and T. J. Richmond.** 1998. DNA binding within the nucleosome core. Curr. Opin. Struct. Biol. **8:**33–40.
21. **Luo, K., M. A. Vega-Palas, and M. Grunstein.** 2002. Rap1-Sir4 binding independent of other Sir, yKu, or histone interactions initiates the assembly of telomeric heterochromatin in yeast. Genes Dev. **16:**1528–1539.
22. **Muthurajan, U. M., Y. Bao, L. J. Forsberg, R. S. Edayathumangalam, P. N. Dyer, C. L. White, and K. Luger.** 2004. Crystal structures of histone Sin mutant nucleosomes reveal altered protein-DNA interactions. EMBO J. **23:**260–271.
23. **Ng, H. H., Q. Feng, H. Wang, H. Erdjument-Bromage, P. Tempst, Y. Zhang, and K. Struhl.** 2002. Lysine methylation within the globular domain of histone H3 by Dot1 is important for telomeric silencing and Sir protein association. Genes Dev. **16:**1518–1527.
24. **Park, J. H., M. S. Cosgrove, E. Youngman, C. Wolberger, and J. D. Boeke.** 2002. A core nucleosome surface crucial for transcriptional silencing. Nat. Genet. **32:**273–279.
25. **Rusche, L. N., A. L. Kirchmaier, and J. Rine.** 2002. Ordered nucleation and spreading of silenced chromatin in Saccharomyces cerevisiae. Mol. Biol. Cell **13:**2207–2222.
26. **Rusche, L. N., A. L. Kirchmaier, and J. Rine.** 2003. The establishment, inheritance, and function of silenced chromatin in Saccharomyces cerevisiae. Annu. Rev. Biochem. **72:**481–516.
27. **Schnell, R., and J. Rine.** 1986. A position effect on the expression of a tRNA

gene mediated by the SIR genes in *Saccharomyces cerevisiae*. Mol. Cell. Biol. **6:**494–501.

28. **Schwarz, P. M., A. Felthauser, T. M. Fletcher, and J. C. Hansen.** 1996. Reversible oligonucleosome self-association: dependence on divalent cations and core histone tail domains. Biochemistry **35:**4009–4015.
29. **Schwarz, P. M., and J. C. Hansen.** 1994. Formation and stability of higher order chromatin structures. Contributions of the histone octamer. J. Biol. Chem. **269:**16284–16289.
30. **Singer, M. S., A. Kahana, A. J. Wolf, L. L. Meisinger, S. E. Peterson, C. Goggin, M. Mahowald, and D. E. Gottschling.** 1998. Identification of high-copy disruptors of telomeric silencing in Saccharomyces cerevisiae. Genetics **150:**613–632.
31. **Smith, J. S., and J. D. Boeke.** 1997. An unusual form of transcriptional silencing in yeast ribosomal DNA. Genes Dev. **11:**241–254.
32. **Smith, J. S., C. B. Brachmann, L. Pillus, and J. D. Boeke.** 1998. Distribution of a limited Sir2 protein pool regulates the strength of yeast rDNA silencing and is modulated by Sir4p. Genetics **149:**1205–1219.
33. **Sternberg, P. W., M. J. Stern, I. Clark, and I. Herskowitz.** 1987. Activation of the yeast HO gene by release from multiple negative controls. Cell **48:** 567–577.
34. **Straight, A. F., W. Shou, G. J. Dowd, C. W. Turck, R. J. Deshaies, A. D. Johnson, and D. Moazed.** 1999. Net1, a Sir2-associated nucleolar protein required for rDNA silencing and nucleolar integrity. Cell **97:**245–256.
35. **Thompson, J. S., M. L. Snow, S. Giles, L. E. McPherson, and M. Grunstein.** 2003. Identification of a functional domain within the essential core of histone H3 that is required for telomeric and HM silencing in Saccharomyces cerevisiae. Genetics **163:**447–452.
36. **van Holde, K. E., and W. O. Weischet.** 1978. Boundary analysis of sedimentation-velocity experiments with monodisperse and paucidisperse solutes. Biopolymers **17:**1387–1403.
37. **van Leeuwen, F., P. R. Gafken, and D. E. Gottschling.** 2002. Dot1p modulates silencing in yeast by methylation of the nucleosome core. Cell **109:**745–756.
38. **Wechser, M. A., M. P. Kladde, J. A. Alfieri, and C. L. Peterson.** 1997. Effects of Sin^- versions of histone H4 on yeast chromatin structure and function. EMBO J. **16:**2086–2095.